

Anomeric Orbital and Steric Control in Static Conformations and Systems Dynamics: Rotations of Methoxy Groups in 2,2-Dimethoxypropane and Similar Crystallographic COCOC Fragments

Aliette Cossé-Barbi and Jacques-Emile Dubois*

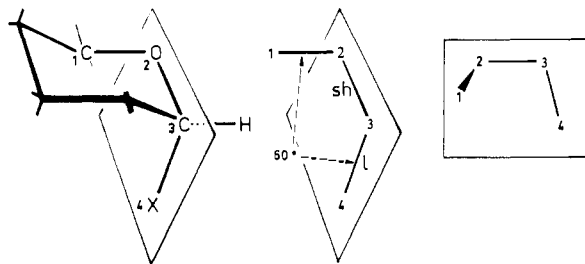
Contribution from the Institut de Topologie et de Dynamique des Systèmes, Université Paris VII, Associé au C.N.R.S., 75005 Paris, France. Received August 9, 1985.

Revised Manuscript Received October 20, 1986

Abstract: The analysis of X-ray data of 546 COCOC molecular fragments extracted from the Cambridge Crystallographic Data Base is associated with MO calculations on dimethoxypropane, conformational INDO map and MO optimization of structural parameters. This population study examines the complex monitoring, through electronic and steric control, of the anomeric effect, in endo plus exo anomeric situations. The two torsion angles of the COCOC fragment ($C_1O_2C_3O_4C_5$) are shown to be the proper conformational mapping tool for 3D molecular investigation. Sixty-six percent of the acyclic fragments with an sp^3 anomeric C_3 carbon show structures having the C_2 symmetry. Anomeric effects of both oxygens exist in most fragments with a quaternary or a secondary C_3 carbon, but the variation in torsion angle is very broad ($\bar{\phi}_1 = 60.11^\circ$ with a standard deviation $\sigma = 9.3^\circ$). Conformational changes and anomeric effect discrepancies are greater when the central carbon is a tertiary one. For cyclic fragments with a tertiary C_3 carbon, there is a wide dispersion of one of the torsion angles: ϕ_{exo} for the six-membered rings ($\bar{\phi}_{exo} = 77^\circ$, $\sigma = 19^\circ$) and ϕ_{endo} for five-membered rings ($\bar{\phi}_{endo} = 104^\circ$, $\sigma = 11.3^\circ$), while in contrast, the other torsion angle is close to 60° (or 180°). This is the result of a conformational strain hindering the characteristic orbital alignments typical of the endo and exo anomeric effects. The endo anomeric effect is found in about 56% of the pyranosides. For labile furanoses, the equatorial conformers are largely handicapped (76% of the alkoxy groups lie between the axial and bisecting positions with respect to the five-membered ring). No correlation was found between CO bond lengths or COC bond angle and torsion angles. In contrast the bond angle OCO at the anomeric center is very sensitive to conformational variation (11° variation between double anomeric structures and nonanomeric structures). The structure correlation method suggests interconversion pathways between conformers of C_2 symmetry which avoid any strong interaction between alkoxy groups. One peripheral pathway associates two correlated disrotations of alkoxy groups with a stepwise rotation of these groups. The interconversion energy for this mechanism is estimated at 1.6 kcal/mol.

The anomeric effect¹⁻³ is associated with the preference of electronegative substituents to assume axial rather than expected equatorial positions at the anomeric carbon in pyranose rings. This conformational situation, unusual in hydrocarbon rings, has been attributed to the presence of two electronegative atoms on a carbon atom. Although discovered in carbohydrate chemistry, its interpretation is based on the study of simple aliphatic model compounds containing the local and minimal substructure COCOC. The anomeric effect was first explained in terms of dipolar electrostatic repulsion and then by an $n \rightarrow \sigma^*$ overlapping between a free electron pair of oxygen and the antibonding σ^* orbital of the neighboring C-X bond (X = electronegative atom).⁴ This kind of stereoelectronic control has long been invoked⁵ to explain certain aspects of methanol and dimethyl ether physical chemistry,⁶ such as the differences in bond lengths and force constants of the CH bonds^{7,8} inside and outside the symmetry plane (COH for

methanol or COC for dimethyl ether). In fact $n \rightarrow \sigma^*$ and dipole-dipole interaction reinforce each other, but the former is now thought to be more important. This overlapping requires a well-defined alignment of orbitals and would stabilize the gauche conformation of the four atoms $C_1O_2C_3X_4$ (dihedral ϕ angle = $\pm 60^\circ$). The requirement that the C_3X_4 bond and a free orbital of the O_2 oxygen be anti-parallel would then account for the shortening^{4,9,10} of the internal C_3O_2 bond, the lengthening of the C_3X_4 bond, and the modification of the hybridization of the O_2 atom and of the anomeric C_3 carbon which would then acquire a more pronounced s character.



This model of the anomeric effect generally refers to very simple structures with weak steric interactions. The reality is very different. Over a large population, including more complex

(1) Edwards, J. T. *Chem. Ind. (London)* **1955**, 1102. Lemieux, R. U.; Chu, N. J. Presented at the 133rd National Meeting of the American Chemical Society, San Francisco, 1958; paper 31N. Lemieux, R. U. *Pure Appl. Chem.* **1971**, *25*, 527.

(2) Kirby, A. J. *The Anomeric Effect and Related Stereoelectronic Effects at Oxygen*; Springer Verlag: Berlin, 1983.

(3) Deslongchamps, P. *Stereoelectronic Effects in Organic Chemistry*; Wiley: New York, 1983.

(4) Romers, C.; Altona, C.; Buys, H. R.; Havinga, E. *Topics in Stereochemistry*; Eliel, E. L., Allinger, N. L., Eds.; Wiley Interscience: New York, London, Sydney, Toronto, 1969; Vol. 4, p 39.

(5) Krueger, P. J.; Jan, J.; Wieser, M. J. *Mol. Struct.* **1970**, *5*, 375.

(6) Freymann, R.; Gueron, J. C. R. *Hebd. Seances Acad. Sci.* **1937**, *205*, 859. Roche, D.; Marcou, A.; Freymann, R. C. R. *Hebd. Seances Acad. Sci.* **1971**, *272*, 1052. Taillandier, E. C. R. *Hebd. Seances Acad. Sci., Ser. B* **1970**, *271*, 693. Perchard, J. P.; Forel, M. T.; Josien, M. L. *J. Chim. Phys.* **1964**, *61*, 632. Henbest, H. B.; Meakins, G. D.; Nicholls, B.; Wagland, A. A. *J. Chem. Soc.* **1957**, 1462. Sauer, O.; Janin, A.; Lavalley, J. C.; Sheppard, N. C. R. *Hebd. Seances Acad. Sci., Ser. B* **1973**, *276*, 725. Hollenstein, H.; Gunthard, Hs. H. *Spectrochim. Acta, Part A* **1971**, *27*, 2027. Lucazeau, G.; Novak, A. *Spectrochim. Acta, Part A* **1969**, *25*, 1615. Lucazeau, G.; Novak, A. *J. Chim. Phys.* **1970**, *67*, 1614; **1971**, *68*, 252.

(7) Serrallach, A.; Meyer, R.; Gunthard, Hs. H. *J. Mol. Spectrosc.* **1974**, *52*, 94.

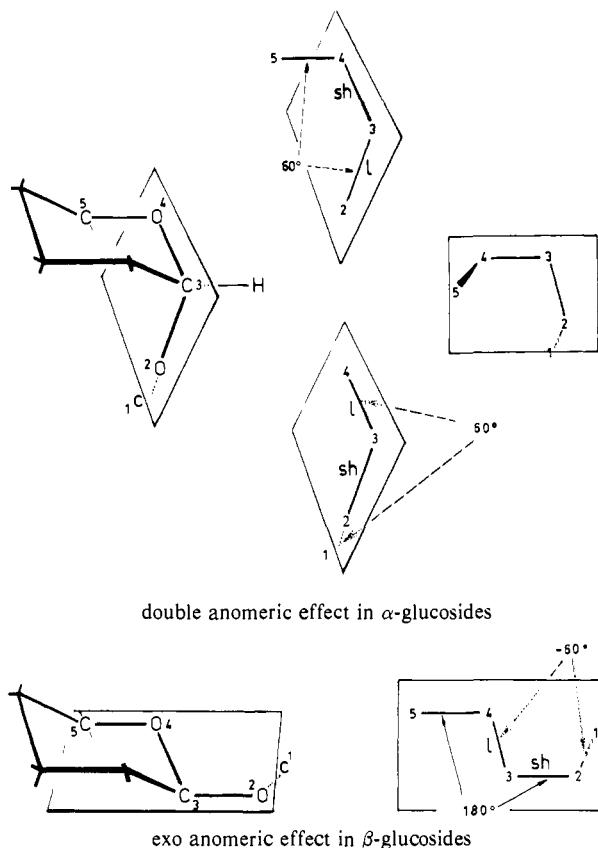
(8) Labarbe, P.; Forel, M. T.; Bessis, G. *Spectrochim. Acta, Part A* **1968**, *24*, 2165. Allan, A.; McKean, D. C.; Perchard, J. P.; Josien, M. L. *Spectrochim. Acta, Part A* **1971**, *27*, 1409.

(9) Jeffrey, G. A.; Berman, H. M.; Chu, S. C. *Science (Washington, D. C.)* **1967**, *157*, 1546. Sundaralingam, M. *Biopolymers* **1968**, *6*, 189. Fuchs, B.; Goldberg, I.; Shmueli, Y. *J. Chem. Soc., Perkin Trans. 2* **1972**, 357. Perez, S.; Marchessault, R. *Carbohydr. Res.* **1978**, *65*, 114. Tvaroska, J.; Kozar, T. *Carbohydr. Res.* **1981**, *90*, 173; *Chem. Z.* **1981**, *35*, 425. Van Alsenoy, C.; Schafer, L.; Scarsdale, J. N.; Geise, H. J. *J. Mol. Struct.* **1981**, *76*, 349.

(10) Jeffrey, G. A.; Pople, J. A.; Binkley, S.; Vishveshwara, S. *J. Am. Chem. Soc.* **1978**, *100*, 373.

structures, Fuchs et al.¹¹ have observed a remarkable dispersion of the values of structural parameters: r distances, θ bond angles, and torsion angles. This dispersion of the test values of the anomeric effect needs a more systematic survey of larger sets of data.

In the α - and β -glucosides, the four COCX atoms are in fact integrated in a longer chain (hereafter the substructure SS) of five atoms, $C_1O_2C_3O_4C_5$, centered on the anomeric carbon C_3 . This chain is capable of showing two anomeric effects: an endo anomeric effect (with a torsion angle $\phi_{\text{endo}} = O_2C_3O_4C_5 \approx \pm 60^\circ$) and an exo anomeric effect (with a torsion angle $\phi_{\text{exo}} = C_1O_2C_3O_4 \approx \pm 60^\circ$). These two endo and exo anomeric effects exist in α -glucosides and have opposing influences on the structural parameters. The result is such a fine modification of the r and θ parameters that only information relating to torsion angles supplies a test which can be used despite its great variability.



Structures in glucosides, although doubly anomeric of C_2 symmetry (exo and endo torsion angles equal in absolute value to 60° and with opposite signs), are destabilized, and one is led to invoke, together with stereoelectronic arguments, the influence of nonbonded interaction (steric effects) among the atoms of the SS.¹²

We felt that these problems could be approached by considering the COCOC substructure as a simplified two rotor system OMe or OR placed in a COC planar framework. We might expect the COCOC substructure to display an interconnection of conformational effects somewhat similar to that observed in other systems where the interaction of two chemical rotors is at work: static and dynamic gear effects,¹³ correlated disrotation or conrotation,¹⁴

and stepwise mechanisms.¹⁵ This dynamic approach should enable us to make a better assessment of the respective weights of stereoelectronic and steric effects.

In this paper, we present some results concerning the simplified situation of two OMe (or OR) chemical rotors placed in a planar OCO framework. We specify the static and dynamic conformational aspects of this system by combining a semiempirical quantum chemical calculation on a model molecule with the analysis of X-ray data retrieved from the Cambridge Crystallographic Data Base.¹⁶

We use the structure correlation method¹⁷ as the general approach for extracting dynamic information from crystallographic data. According to this method, a distribution of sample points corresponding to observed crystal structures will tend to concentrate in low-lying regions of the potential energy surface: the interaction energy between the molecular fragment concerned and its various crystal or molecular environments is regarded as a small perturbation relative to the total molecular energy. Applied to a broad set of compounds, the structural correlation method allows one to calculate interconversion pathways between conformers. We apply it here to 546 fragments having the COCOC substructure of acetals in common: 89 fragments are acyclic and 457 are cyclic and liable to show the endo and exo anomeric effects of sugars. We shall include information gleaned from neutron and X-ray data unfortunately carried out only on the ϕ_{exo} angle, in a basic paper by Jeffrey et al.¹⁰ and from a study of a population of data recently published by Fuchs et al.¹¹ For our dynamic investigation on a much larger population of compounds, we will need both ϕ_{endo} and ϕ_{exo} torsion angle values.

However, as was pointed out by Dunitz and Bürgi,¹⁷ the pathways deduced by analyzing X-ray results must be confirmed by supplementary information, since it is not always easy to decide whether to interpret them as characteristic of the substructure (COCOC in this case) or as response pathways linked to a specific constraint of the intramolecular environment, such as cyclization. In our study, such supplementary information is sought by a quantum calculation on a model molecule, dimethoxypropane. This compound should mimic the substructure encountered in substituted pyranoses (quaternary anomeric C_3 carbon), and we shall also show that it is a better approximation to the normal pyranoses not substituted at their tertiary anomeric C_3 carbon. We believe that it could present some advantages over dimethoxymethane which was used in previous studies.^{10,12} Though this is one step further in the model compound strategy to mimic the acetal moiety, the earlier work on dimethoxymethane remains essential in our exploration of the anomeric effect on a wide range of structures.

I. Methods

A. Data Retrieval and Reduction. The experimental information for our analysis was taken from the Cambridge Crystallographic Data Base updated to Jan 1983. We refer the reader to the fundamental articles describing this data base organization.¹⁶ We have adapted the query software to interactive treatment, and this work is described elsewhere.¹⁸

(1) Connectivity Search. This selects structures containing COCOC fragments. In substructure A, the four bonds are acyclic. Carbon C_3 can be quaternary, tertiary, or secondary (i.e., linked to four, three, or two heavy atoms, carbon or heteroatom). Carbons C_1 and C_5 can be substituted or not. In substructures B and C, the four bonds are simple: bonds 12 and 23 are acyclic, while bonds 34 and 45 are cyclic. Carbon

(14) Kwart, H.; Alckman, S. *J. Am. Chem. Soc.* **1968**, *90*, 4482. Mislow, K. *Acc. Chem. Res.* **1976**, *26*, 9. Guenzi, A.; Johnson, A.; Cozzi, F.; Mislow, K. *J. Am. Chem. Soc.* **1983**, *105*, 1438. Kawada, Y.; Twamura, H. *J. Am. Chem. Soc.* **1983**, *105*, 1449.

(15) Berg, U.; Liljefors, T.; Roussel, C.; Sandström, J. *Acc. Chem. Res.* **1985**, *18*, 80.

(16) Allen, F. H.; Bellard, S.; Brice, M. D.; Cartwright, B. A.; Doubleday, A.; Higgs, H.; Hummelink, T.; Hummelin-Peters, B.; Kennard, O.; Motherwell, W. D. S.; Rodgers, J. R.; Watson, D. G. *Acta Crystallogr., Sect. B* **1979**, *35*, 2331. Wilson, S. R.; Huffman, J. C. *J. Org. Chem.* **1980**, *45*, 560.

(17) Bürgi, H. B.; Dunitz, J. D. *Acc. Chem. Res.* **1983**, *16*, 153. Murray-Rust, P.; Bürgi, H. B.; Dunitz, J. B. *J. Am. Chem. Soc.* **1975**, *97*, 921, footnote 1.

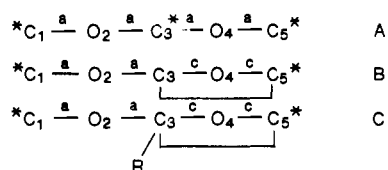
(18) Attias, R.; Sobel, Y.; Couesnon, T.; Cossé-Barbi, A. unpublished results.

(11) Fuchs, B.; Schleifer, L.; Tartakovsky, E. *Nouv. J. Chim.* **1984**, *8*, 275.

(12) Jeffrey, G. A.; Pople, J. A.; Random, L. *Carbohydr. Res.* **1972**, *25*, 117. Electron delocalization, dipole-dipole interactions, and steric effect have been considered in this reference.

(13) Hounshell, W. D.; Iroff, L. D.; Wroczyński, R. J.; Mislow, K. *J. Am. Chem. Soc.* **1978**, *100*, 5212 and references therein. Roussel, C.; Chanon, M.; Metzger, J. *Tetrahedron Lett.* **1971**, 1861. Roussel, C.; Liden, A.; Chanon, M.; Metzger, J.; Sandström, J. *J. Am. Chem. Soc.* **1976**, *98*, 3847. Hounshell, W. D.; Iroff, L. D.; Iverson, D. J.; Wroczyński, R. J.; Mislow, K. *Isr. J. Chem.* **1980**, *20*, 65.

C₃, anomeric, is tertiary in substructure B and quaternary in substructure C. Carbons C₁ and C₅ can carry substituents.



substructures A-C with possible substitutions on carbons C₁, C₃, and C₅

(2) **Visualizing Structures.** Visualizing structures in two dimensions (DARC) and in three dimensions (PLUTO 78) enables one to verify the existence of the fragments sought, to discover the existence of invalid fragments whose connectivity was poorly coded in the Cambridge Data Base, and to eliminate fragments that resemble each other by their connectivity but show different bonds (cyclic or acyclic).

For entries containing more than one COCOC fragment, any erroneous additional fragments are not automatically eliminated by the geometry calculation program (GEOM 78) which makes no provision for bond type. These must be removed by inspection of each individual entry. This is how we excluded the COCOC fragments with four cyclic bonds (2-alkoxy-1,3-dioxanes and 2-alkoxy-1,3-dioxolanes). Four acyclic fragments are retrieved by direct inspection of geometry (geometry calculation program applies to the entire data base), and the connectivity is monitored by PLUTO 78.

(3) **Precision Analysis.** After this selection, we obtain 76 hits corresponding to substructure A, 332 hits corresponding to substructure B, and 72 hits corresponding to substructure C. Of these 480 hits, 91 cannot be used because the atomic coordinates are not stored. Of those remaining, 63 hits lead to 64 entries for substructure A, 269 hits lead to 296 entries for substructure B, and 57 hits lead to 59 entries for substructure C.

Crystallographic and bibliographic information are obtained interactively. The latter is summarized in the supplementary material.

Four acyclic fragments (SS A) and 18 cyclic fragments (SS B) were eliminated because the atomic coordinates were unreliable (error flag!) or because the crystal structure was insufficiently precise for our purpose (reliability index R greater than 0.15). This left 85 fragments for SS A, 370 fragments for SS B, and 75 fragments for SS C.

B. Geometry Calculation and Division Into Subclasses. The geometry calculation is carried out interactively on the answer file resulting from the connectivity search. For each COCOC fragment, we have been careful to specify the four r distances, the three θ valency angles, and the two ϕ_1 and ϕ_2 torsion angles.

In order to precisely evaluate the influence of the intramolecular environment on these nine structural parameters, we divided the fragments into subclasses. The acyclic fragments were divided according to the quaternary, tertiary, or secondary nature of the C₃ anomeric atom and the existence or nonexistence of substituents on the terminal carbons C₁ and C₅. The cyclic fragments corresponding to substructures B and C were divided according to the size of the ring: five or six heavy atoms (C or heteroatom) and, more exceptionally, three, seven, or eight heavy atoms. Bicyclic structures were analyzed separately.

C. Reducing the Useful Conformational Space. The bidimensional space defined by ϕ_1 and ϕ_2 provides an image of stable and unstable conformers and enables us to describe their interconversion. The sym-

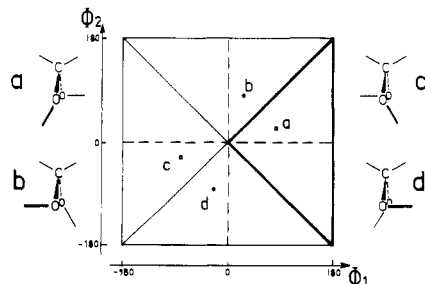
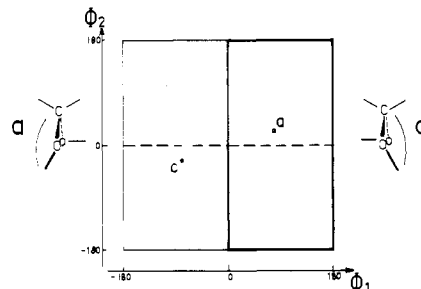


Figure 1. Conformational crystallographic data of acyclic COCOC fragments. MeOCOMe: (●) quaternary C₃ carbon, 35 cases; (○) tertiary C₃ carbon, 8 cases. R₁OCOR₂: (◇) R₁ ≠ H, R₂ ≠ H, Me, 42 cases; (△) gas phases, dimethoxymethane and dimethoxypropane.²¹ Each structure is represented by four points deduced one from the other by symmetries related to axes S₁ and S₂ and to the center of coordinates.

ment conformations. We can say equally well that the conformational space measuring $360^\circ \times 360^\circ$ contains 85×4 points.

The same is not true, however, for the cyclic substructures B and C. The distinction between ϕ_{exo} and ϕ_{endo} angles limits the symmetry of the conformational space which is then isomorphic to group C₂. Only the



substructures B and C: two equivalent rectangular cells measuring $(360^\circ \times 360^\circ)/2$

two points a and c with coordinates $(\phi_{exo}, \phi_{endo})$ and $(-\phi_{exo}, -\phi_{endo})$ will then correspond to identical conformers. A cell measuring $(360^\circ \times 360^\circ)/2$ will then contain all the available information. It will contain 370 points corresponding to the substructure B and 79 corresponding to the substructure C. The dimension space $360^\circ \times 360^\circ$ then contains 370×2 (SS B) and 158 points (SS C).

D. MO Calculations. Calculations are performed on dimethoxypropane by the INDO method.¹⁹ The potential energy surface $E(\phi_1, \phi_2)$ and the associated conformational map are obtained for a model molecule with all bond lengths and bond angles fixed at standard values. The algorithm used adapts numerical cartography programs to chemistry. There are 5-deg steps on the torsion angle. Along the interconversion pathways, the molecular geometries are optimized (18 structural parameters) by using the procedure proposed by Rinaldi.²⁰

II. Crystallographic Data Analysis as Related to Anomeric Effect

A. Conformational Variability of Acyclic COCOC Fragments. The conformational space built on the two torsion angles ϕ_1 (C₁O₂C₃O₄) and ϕ_2 (O₂C₃O₄C₅) is a good tool by which to appreciate the conformational variability of fragments (Figure 1).

substructure A: four equivalent triangular cells within the $360^\circ \times 360^\circ$ space spanned by (ϕ_1, ϕ_2)

metry of this space is isomorphic to C_{2v}, which expresses the symmetry of the OCO frame. The four points $a-d$ represent equivalent general positions (ϕ_1, ϕ_2) that correspond to isometric structures.

A cell measuring $(360^\circ \times 360^\circ)/4$ can thus contain all available information. This cell contains 85 points representing the acyclic frag-

(19) Pople, J. A.; Beveridge, D. L.; Dobosh, P. A. *J. Chem. Phys.* **1967**, *47*, 2026.

(20) Rinaldi, D.; Rivail, J. L. *C. R. Hebd. Seances Acad. Sci., Ser. C* **1972**, *274*, 1664.

(21) Astrup, E. E. *Acta Chem. Scand.* **1973**, *27*, 3271. Astrup, E. E.; Aomar, A. M. *Acta Chem. Scand., Ser. A* **1975**, *A29*, 794.

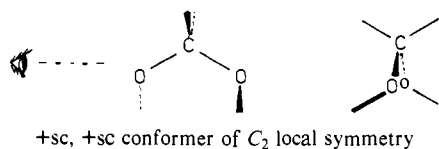
Table I. Occurrence of Antiperiplanar, Antiperiplanar (ap, ap); Synclinal, Synclinal (sc, sc) with Two ϕ_i of the Same Sign (+sc, +sc), or Two ϕ_i of Opposite Signs (+sc, -sc); Synperiplanar, Synclinal (sp, sc); Synclinal, Antiperiplanar (sc, ap); and Synperiplanar, Antiperiplanar (sp, ap) Conformers for Acyclic COCOC Fragments and Mean Values of ϕ_i (deg) and Standard Deviation (σ)

	C_3	total	conformers	$\bar{\phi}_1$ (σ)	$\bar{\phi}_2$ (σ)
MeOCOME	quaternary	35	ap, ap (3)	173.9	173.9 (5.7)
			+sc, +sc (32)	56.2	56.2 (5.8)
	tertiary	8	+sc, +sc (4)	62.5	62.5 (9.5)
			+sc, -sc (3)	69.7 (4.7)	-126 (24.1)
R ₁ OCOR ₂ R ₁ ≠ H R ₂ ≠ H, Me	quaternary	8	sp, sc (1)	12	88
			ap, ap (4)	176.8 ^a	176.8 ^a (2.3)
			sc, ap (2)	52.4 (0.3)	-171.2 (3.5)
			+sc, +sc (2)	56.10	56.10 (3.5)
	tertiary C_3 sp ²	18	ap, ap (16)	176.5 ^a	176.5 ^a (3.2)
			sp, ap (1)	10.6	174
			sp, sc (1)	2	87
	tertiary C_3 sp ³	11	+sc, +sc (1)	49	70
			+sc, -sc (9)	82.6 (4.8)	-136.6 (14.2)
			sc, ap (1)	-85	172
secondary	5	+sc, +sc (5)	76.1	76.1 (5.0)	

^a Absolute values.

Seventy-nine of the 85 acyclic fragments (i.e., 93%) show an sc, sc or an ap, ap (sc = synclinal; ap = antiperiplanar; sp = synperiplanar) conformer in the crystal phase (Table I).

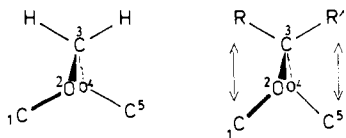
(1) +sc, +sc Conformers. Forty-four of the 67 fragments (i.e., 66%) which have an sp³ C₃ carbon adopt a structure with local C₂ symmetry in the crystal phase. The representative points in Figure 1 are in quadrants 1 and 3 corresponding to ϕ_1 and ϕ_2 angles of the same sign, near the S₁ axis ($\phi_1 = \phi_2$). The ϕ_i mean value is very close to 60° ($\bar{\phi}_i = 60.11^\circ$), but the variation of torsion angles seems very broad (38–84° with a standard deviation $\sigma = 9.3^\circ$).



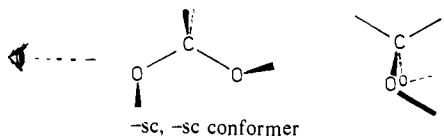
This structure of C₂ symmetry reveals a double anomeric effect of oxygen, since each central C–O bond is antiparallel to one of the free orbitals of the other oxygen.

We must note that the C₃ structures are more readily obtained if the central sp³ carbon is quaternary or secondary (39 of the 44 fragments), i.e., in the COCOC fragments showing a local symmetry at the level of the C₃ acetalic carbon. Among these latter, we observe an increase of the ϕ_i values if the anomeric C₃ center is secondary rather than quaternary (Table I).

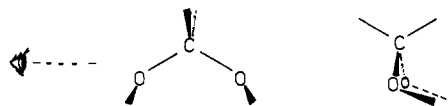
It seems that in these structures where a double anomeric effect is justly suspected, steric effects due to the two substituents R and R' of carbon C₃ block the structure in a situation of smaller ϕ_i angles if the carbon is quaternary. The absence of these substituents allows for greater torsion angles when the anomeric carbon is secondary.



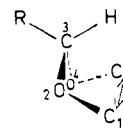
(2) +sc, -sc Conformers. For 12 structures with an sp³ C₃ carbon (i.e., 18%), the representative points belong to quadrants 2 and 4 with ϕ_i angles of opposite signs (+sc, -sc conformers). One of the angles is included between 64° and 91° ($\bar{\phi}_i = 79.4^\circ$; $\sigma = 14^\circ$), while the other varies from -104° to -153°. ($\phi_i = -133.9^\circ$; $\sigma = 20.9$). The anomeric effect is thus approximate for some compounds and limited to only one of the two oxygens.



We must note one nonanomeric +sc, -sc structure whose representative point is close to the S₂ axis ($\phi_1 = -\phi_2$) and whose local symmetry is approximately C_s:

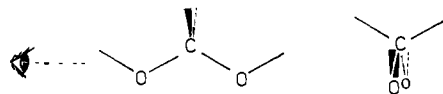


The conformational situation of these 12 +sc, -sc conformers, which all have a tertiary C₃ carbon, confirms the role played by steric effects. The local dissymmetry of carbon C₃ permits a relevant conformational relaxation of interaction C₁R or C₅R by a rotation of carbons C₁ and C₅ on the same side of the plane O₂C₃O₄ (ϕ_1 and ϕ_2 of opposite signs).



However, such a conformational situation tends to diminish the C₁C₅ distance, augmenting the corresponding steric interaction if the absolute values of angles ϕ_i remain close to 60° (anomeric structures). Augmenting angles ϕ_i in absolute value brings about the relaxation of interactions between 1 and 5.

(3) ap, ap Conformers. Twenty-three fragments (16 with an sp² C₃ carbon, i.e., 89%, and 7 with an sp³ C₃ carbon, i.e., 10%) show an antiperiplanar, antiperiplanar conformation ($\phi_1 \approx \phi_2 \approx 180^\circ$) with local C_{2v} symmetry:



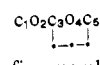
(4) Unusual Structures. For 6 of the 85 fragments (i.e., 7%), the observed conformer is neither sc, sc nor ap, ap. Three sc, ap conformers are similar to β conformers of glucosides. Two compounds are very special with one ϕ_i near 0° and the other near 90°. Their 3D structure is shown in the supplementary material.

B. Conformational Variability in Alkoxy-Substituted Rings. Figure 2 summarizes crystallographic data for 439 cyclic fragments including fragments with a tertiary C₃ carbon (such as glucosides) or with a quaternary C₃ carbon.

In alkoxy-substituted rings, and despite the inclusion of a part of the COCOC substructure in a ring, we must note a large conformational variation, whether the carbon at the center of the fragment is tertiary (360 fragments, Figure 2a) or quaternary (79 fragments Figure 2b).

(1) Tertiary C₃ Carbon. Conformational changes mainly affect, and considerably so, one of the two ϕ_i angles, the other angle remaining at a value near 60° or 180°. Moreover, the ϕ_{exo} (ϕ_1) angle is the variable which undergoes the greatest variations for

Table II. Mean Values of Torsion Angles (and Standard Deviation) Related to Conformers (deg)

	C ₃	conformers	no.	ϕ_{endo}	ϕ_{exo}
six-membered rings	tertiary	+sc, +sc (α)	178	63.8 (7.9)	77.0 (19.4)
		ap, sc (β)	127	176.7 (5.6)	77.2 (18.4)
$\text{C}_1\text{O}_2\text{C}_3\text{O}_4\text{C}_5$ 	quaternary	+sc, +sc (α)	4	66.7 (3.6)	54.5 (5.6)
		ap, sc (β)	10	175.6 (2.9)	61.7 (4.2)
five membered rings	tertiary	+sc, +sc	28	103.8 (11.3)	72.4 (6.4)
		quaternary	25	95.9 (10.7)	52.8 (13.4)
		+sc, -sc	17	-125.8 (14.4)	55.5 (13.3)

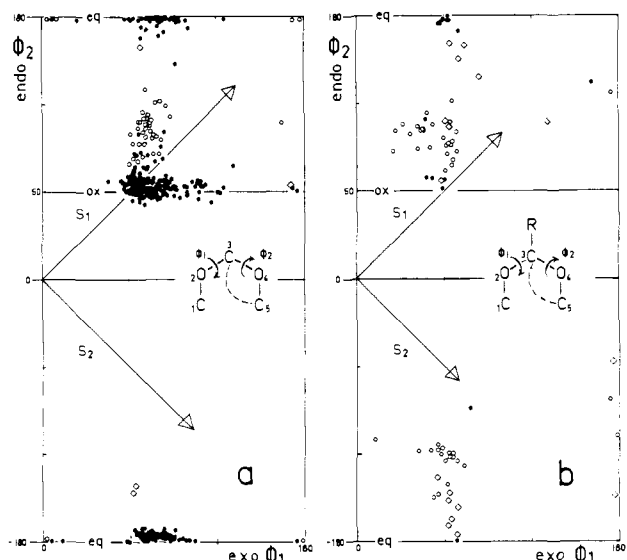


Figure 2. Conformational crystallographic data for cyclic fragments (a) with a tertiary C₃ carbon and (b) with a quaternary C₃ carbon; (○) five-membered rings, (●) six-membered rings, (◇) others.

the six-membered rings, the ϕ_{endo} (ϕ_2) being this variable for the five-membered rings.

(a) **Six-Membered Rings** (● in Figure 2a). For most of the population of 316 fragments the ϕ_{endo} angle takes on values very close to 60° or 180°, thus testifying to the rigidity of the chair conformations of the six-membered rings (see also mean values and standard deviations in Table II). The alkoxy group is equatorial (ϕ_2 between 165° and 180° and between -170° and 180°) for 40.2% of the population and axial (ϕ_2 between 50° and 80°) for 56.3%. (This mean contribution of the α form is slightly overestimated: for a few structures, the anomeric oxygen is disordered and only the α form was stored in the data base.) Only 11 fragments have a ϕ_{endo} angle outside these intervals. As observed long ago, the axial form (such as α -glycosides) which manifests the endo anomeric effect of O₄ oxygen is more frequent than the equatorial form (such as β -glycosides).

Conformational changes are notable in the C₁C₂ exo bond situation with respect to the rigid chair: for 121 fragments taken from the 127 equatorial forms, ϕ_{exo} varies from 54° to 105°, while for 174 taken from 178 axial forms, ϕ_{exo} varies from 54° to 125°. We thus go from situations where the exo anomeric effect of oxygen O₂ seems indisputable ($\phi_1 \approx 60^\circ$) to conformers where it is doubtful ($\phi_1 \approx 90^\circ$) or nonexistent ($\phi_1 \approx 120^\circ$). This observation of a wide dispersion of ϕ_{exo} angles (standard deviations = 19°), based here on 316 fragments, generalizes the results of Jeffrey et al.¹⁰ on 34 fragments and of Fuchs et al.¹¹ on 111 fragments. These last authors attribute the large mean value of ϕ_{exo} (here 77°) to the nonequivalence of pairs²²⁻²⁴ of the exo oxygen

(22) The energetic nonequivalence of the oxygen lone pairs shown by photoelectron spectroscopy²³ seems to be a significant factor in determining the anomeric effect.²⁴

(23) Sweigart, D. W.; Turner, D. W. *J. Am. Chem. Soc.* **1972**, *94*, 5599 and references therein.

(24) David, S.; Eisenstein, O.; Hehre, W. J.; Salem, L. *J. Am. Chem. Soc.* **1973**, *95*, 3806. Eisenstein, O.; Nguyen, T. A.; Jean, Y.; Devaquet, A.; Cantacuzene, J.; Salem, L. *Tetrahedron* **1974**, *30*, 1717.

which could achieve better overlapping with orbital σ^* of the endocyclic bond C₃O₄ compatible with the environment. In any case, the anomeric effect is neither as simple nor as evident as might have been expected in such compounds.

(b) **Five-Membered Rings** (○ in Figure 2a). The dihedral ϕ_{endo} angle varies greatly (standard deviation = 11°), illustrating the well-known flexibility of five-atom rings which can adopt half-chair (C₂), envelope (C₃), and "in between" forms along the pseudorotational circuit. With regard to the ring the alkoxy group adopts all positions between the axial ($\phi_{\text{endo}} = 80^\circ$) and the bisecting ($\phi_2 = 110$ –130°) with the exclusion of equatorial positions ($\phi_2 \approx -160^\circ$). (These dihedral angles, $\pm 80^\circ$ and $\pm 160^\circ$, are classical for axially oriented and equatorially oriented substituents in the puckered part of the five-membered rings. Values near $\pm 110^\circ$ and $\pm 130^\circ$ are known for bisecting substituents in the planar part.⁴) In consequence, in these flexible rings, we note a conformational preference avoiding, as in six-membered rings, the equatorial positions of substituents.

Oddly enough, the position of bond C₁O₂ seems more sharply defined (ϕ_{exo} between 59° and 87° with a mean value of 72° obtained with a standard deviation $\approx 6^\circ$). It produces an approximate exo anomeric effect, whatever the five-membered ring conformation (and, consequently, the O₄ endo anomeric effect). The exo bond seems to adapt its spatial position to the intracyclic modifications of the five-atom ring.

As in six-membered rings, the most variable torsion angle (here ϕ_{endo}) varies from 60° or 80° to greater values.

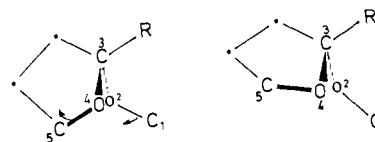
(2) **Quaternary C₃ Carbon** (Figure 2b). Most of this population is formed by five-membered rings. In these more crowded structures, we must note important variations of both ϕ_{exo} and ϕ_{endo} .

(a) **Five-Membered Rings.** ϕ_{endo} values bear witness to the flexibility of the ring. As for C₃ tertiary carbon ϕ_{endo} varies from 70° to 110° ($\bar{\phi}_{\text{endo}} = 96^\circ$); the alkoxy group adopts all orientations between an axial one to a bisecting one. But, ϕ_{endo} can also assume values from -110° to -150° corresponding to alkoxy groups rotated from bisecting to equatorial positions ($\bar{\phi}_{\text{endo}} = -126^\circ$). The other (axial or bisecting) position is taken by the R substituent which is also an alkoxy group in only 4 fragments of the 45. *Five-membered rings with quaternary carbon C₃ thus clearly escape the endo anomeric effect.*

In contrast, the values of ϕ_{exo} are more clearly grouped between 45° and 60° (32 of the 45 cases). Mean values of ϕ_{exo} are closer to 60° than those obtained for alkoxy rings with tertiary C₃ carbon.

It is also interesting to note that if $|\phi_2|$ varies from 60° or 110° toward larger values (Figures 1 and 2a), then $|\phi_1|$ takes on values smaller than 70°.

This observation of low ϕ_{exo} values is subject to steric interpretation. When the alkoxy group moves from the axial position ($\phi_{\text{endo}} = 80^\circ$) to the bisecting position ($\phi_{\text{endo}} = 110^\circ$),

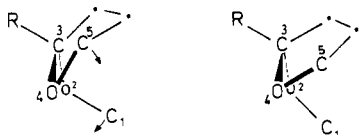


there is a greater occurrence of low ϕ_{exo} values: C₁ draws closer to the O₂C₃O₄ plane. These lower values limit interactions RC₁ of atom C₁ and its substituents with substituent R, while not increasing the interactions of C₁ and its substituents with the ring and in particular atom C₅.

Table III. Anomeric Effects of O₂ and O₄ Oxygens Related to Mean Values of C₃O₂ and C₃O₄ Bond Distances (Å) and C₁O₂C₃, C₃O₄C₅, and O₂C₃O₄ Bond Angles (deg)

C ₃		conformers	anomeric effects	$r(\text{C}_3\text{O}_4)-r(\text{C}_3\text{O}_2)$	r diff.	$\angle\text{C}_3\text{O}_4\text{O}_5-\angle\text{C}_1\text{O}_2\text{C}_3$	\angle diff.	$\angle\text{O}_2\text{C}_3\text{O}_4$	\angle diff.		
acyclic	quaternary	+sc, +sc (34)	2	1.405		116.116		112.52			
	tertiary sp ³ tertiary sp ²	ap, ap (7)	0	1.421	0.016	115.321	0.795	100.56	11.96		
		+sc, -sc (12)	≈ 1					107.16			
		ap, ap (16)	0				106.60				
	secondary	sp, sc (1) +sc, +sc (5)	2	1.420		116.491		120.97	14.37		
								111.46			
C ₃		conformers	anomeric effects	$r(\text{C}_3\text{O}_4)$ endo	$r(\text{C}_3\text{O}_2)$ exo	r diff.	$\angle\text{C}_3\text{O}_4\text{O}_5$ endo	$\angle\text{C}_1\text{O}_2\text{C}_3$ exo	\angle diff.	$\angle\text{O}_2\text{C}_3\text{O}_4$	\angle diff.
six-membered rings	tertiary	+sc, +sc α (178)	endo, ≈ exo	1.416	1.411	0.005	114.124	114.713	-0.590	111.371	
	quaternary	ap, sc β (127)	≈ exo	1.423	1.394	0.029	112.243	115.472	-3.229	107.419	3.95
+sc, +sc α (4)		endo, exo		1.430	1.408	0.022	111.995	116.680	-4.685	110.667	3.69
five-membered rings	tertiary	ap, sc β (10)	exo	1.404	1.394	0.010	112.871	116.802	-3.931	106.975	
		+sc, +sc (28)	≈ exo	1.418	1.408	0.098	109.892	113.143	-3.252	111.043	
	quaternary	+sc, +sc (25)	exo	1.420	1.410	0.01	109.644	116.855	-7.211	110.457	
		+sc, -sc (17)	exo	1.444	1.392	0.052	108.504	117.142	-8.638	109.887	

Similarly, the rotation of the alkoxy group from the approximately equatorial position ($\phi_2 \approx -160^\circ$) to the bisecting position ($\phi_2 \approx -110^\circ$)



increases the occurrence of low ϕ_{exo} values: C₁ draws closer to the plane O₂C₃O₄. These low ϕ_{exo} values limit the interaction of atom C₁ and of its substituents with the ring and particularly the atom C₅, while they do not increase the interactions of atom C₁ and its substituents with substituent R.

Moreover, we note two unusual structures with ϕ_{exo} near 0° and ϕ_{endo} between 90° and 100° (supplementary material).

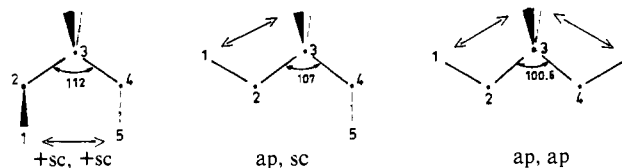
(b) **Whole Population.** Concerning the whole population of cyclic fragments with a quaternary C₃ carbon, 60 fragments from the 79 (76%) exhibit an approximate exo anomeric effect (ϕ_{exo} from 47° to 80°). Both exo and endo anomeric effects are complied with in 17 fragments (21%). In these alkoxy-substituted rings, a clear competition between electronic and steric factors occurs, the crowding at the C₃ carbon level being able to suppress any anomeric effect.

C. Structural Parameters of COCOC Fragments as a Probe for Anomeric Effects? Using the dihedral angles as the only criterion for the existence of anomeric effects, the destabilization of equatorial forms in rings with tertiary C₃ acetalic carbons seems to be confirmed. It is, however, difficult to say if *spreading* (and the deviation from 60°) of ϕ_{endo} values can be explained by a variable dissymmetrical role played by the two O₄ oxygen pairs (which "sees" a dissymmetrical tertiary carbon) or else by steric factors which would compete with the stereoelectronic effects. The problem is complex as the anomeric effect relates the position of CO bonds to that of lone pairs, and only the former are found by X-ray crystallography. Lone pairs are diffused elements subjected to deformation, difficult to localize in space, especially when angles COC differ from their standard value (109°.28').

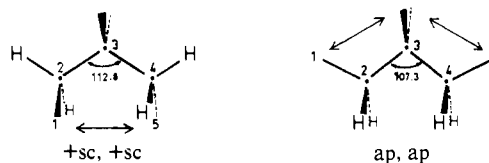
If torsion angles are imperfect indicators of orbital alignment, the shortening of internal CO distances, the lengthening of external CO distances, and the variation of bond angles COC could provide more information. However, the mean values of CO distances and of COC angles (Table III) do not play this role. Indeed one observes a wide dispersion of bond angle values and of internal CO distances concomitant with the dispersion of torsion angles (see also ref 11). We obtained no significant correlation between the torsion angles and distances C₃O₂ and C₃O₄ (or angles C₁O₂C₃ and C₃O₄C₅). This observation should be related to those of Kirby

and co-workers on the role played by the electron demand of exocyclic groups.²⁵

Only the central angle O₂C₃O₄ appears particularly sensitive to the conformational variation. An important angle reduction is observed (12° or 14°) when going from conformation +sc, +sc or sp, sc to the open conformation ap, ap. The variation is smaller (3.5–4°) when we compare conformers +sc, +sc and ap, sc of α- and β-glucosides.



We do not feel that such important angle reduction can be interpreted only by the electronic effect of free pairs of anomeric oxygens. We see the influence of steric interactions involving the substituents of carbon C₃ as well as carbon C₁ and C₅ and their substituents. This is supported by the crystallographic results of compounds related to 3,3-dimethylpentane CH₃CH₂C(CH₃)₂CH₂CH₃. In going from conformation +sc, +sc to conformation ap, ap, the average value of the central angle diminishes by ≈ 5°.



Normally, repulsion interactions involving substituent hydrogens of atoms 2 and 4 limit angle reduction in these hydrocarbons. In dimethoxypropane, the absence of atoms on the free pair sites can partly explain the greater angle reduction.

III. Interconversion Mechanisms between Conformers of C₂ Symmetry

A. Crystallographic Pathways. In conformity with the structural correlation method,¹⁷ structures observed in crystals tend to concentrate in the lower areas of the potential energy surface characteristic of the substructure.

Using the potential symmetry of the COCOC moiety and without separating cyclic and acyclic fragments as in Figures 1

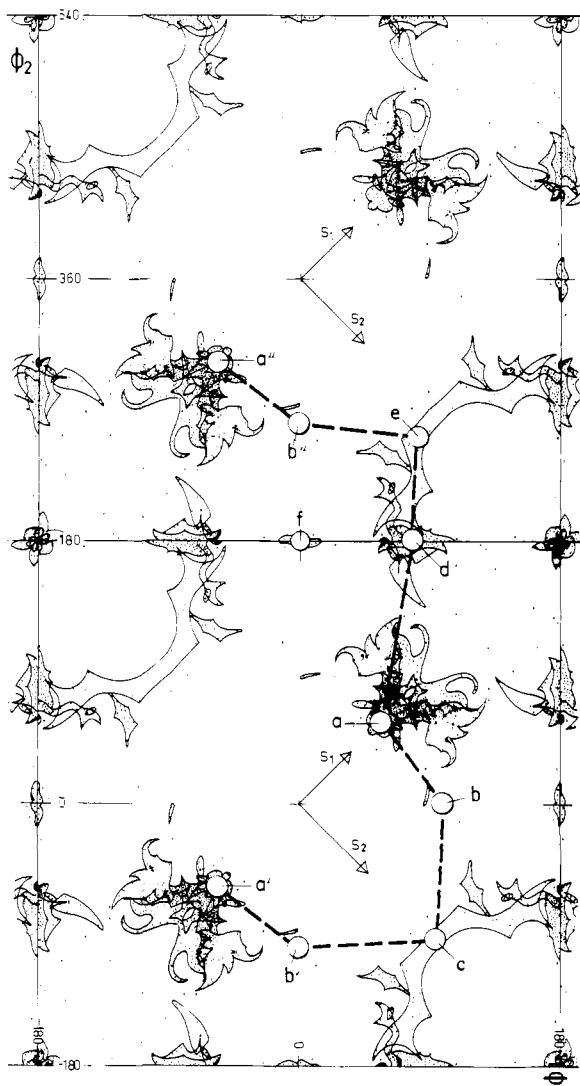


Figure 3. Interconversion pathway estimation from conformational crystallographic data of acyclic and cyclic fragments. The lines outline as closely as possible clusters of points in Figures 1 and 2 with their real density (experimental points).

and 2, one could expect the distribution of conformational energy minima to correspond to that shown in Figure 3. Such minima are not actually connected by continuous sequences corresponding to the gradual deformation of the fragment. We nonetheless feel confident that these crystallographic (and thus static) results imply the existence of several interconversion pathways between equivalent conformers of C_2 symmetry.

(1) Peripheral Pathway. One of these is a peripheral interconversion pathway $abcb'a'$ avoiding the constrained structure ($\phi_1 = \phi_2 = 0^\circ$). If we exclude the clusters of points corresponding to the minimum of C_2 symmetry (ϕ_1 and ϕ_2 from 45° to 65°), this peripheral pathway links (Figure 4) 28×4 conformational situations of the COCOC fragment frozen in a particular acyclic or cyclic environment.

(2) Lateral Pathway. The other pathway $adeb''a''$ may be called a "lateral" one. It also avoids the central constrained structure ($\phi_1 = \phi_2 = 0^\circ$) maintaining, in a first step, the constancy of one angle ϕ and, in a second step, following the above peripheral pathway (Figure 3). Without the two minima corresponding to α - and β -glycoside structures, this pathway links about 100×4 conformational situations of the COCOC substructure.

It is important that, on both pathways, we find acyclic and cyclic fragments as well as fragments with tertiary or quaternary C_3 carbons.

B. Theoretical Pathways: MO Calculations. The two pathways for interconversion depend on the existence of four exceptional

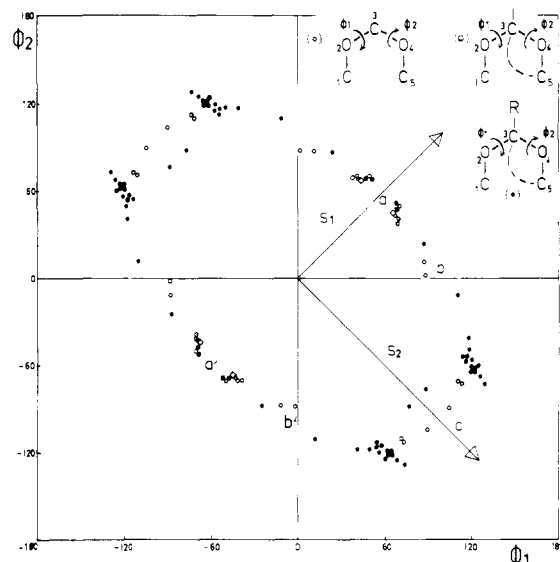


Figure 4. Peripheral pathway drawn by 28×4 COCOC fragments frozen in a particular intra- and intermolecular environment.

structures previously mentioned (sections II-A.4 and III-A.2) with one ϕ_i near 0° and the other near 90° .

It is not certain whether these pathways, based on crystallographic results, are characteristic of the COCOC substructure or are partly created by the extra constraint imposed by the substituents and the ring formation.¹⁷ An a priori calculation of the conformation map on a model molecule should be useful in making a decision.

Which is the most relevant substructure or the best conformational map for pathway elucidation?

(1) Model Compound: Acyclic Fragments as Models for Cyclic Ones. Acyclic compounds like dimethoxymethane, methanediol, were considered model systems for the conformational analysis of carbohydrates.^{10,12} The comparison between Figure 1 and Figure 2 shows how acyclic fragments can play this role.

There are two clear similarities between Figures 1 and 2: the emptiness of the central area and a heavy density of points on the axis for $\phi_1 \approx \phi_2 \approx 60-80^\circ$. C_2 local symmetry structures are obtained in both cyclic and acyclic series, but the correspondence does not follow the hindrance of carbon C_3 . These C_2 symmetry structures are revealed by the secondary and quaternary carbons in acyclic series and by tertiary carbons in cyclic series and are more systematic in acyclic series. Moreover, their deformations are very different in the two series. In Figure 2a, the tails prolonging the clouds of points parallel to the axes for ϕ angles near $60-80^\circ$ have no correspondence in Figure 1 which shows a deformation of the cloud along the S_1 axis.

As might have been expected, the closing of a ring introduces specific conformational elements. It is, however, curious that the very particular dissymmetry introduced by the ring finds no correspondence in the acyclic structures with tertiary carbon C_3 .

In Figures 1 and 2b, one finds a notable spreading of points in a band parallel to the axis of the ordinates, similar although a little shifted ($\phi_1 = 75-85^\circ$, $\phi_2 < -110^\circ$ for cyclic fragments, Figure 1; $\phi_1 = 47-80^\circ$, $\phi_2 < -110^\circ$ for cyclic fragments, Figure 2b). However, this correspondence between cyclic and acyclic fragments is not obtained for a degree of substitution comparable to the anomeric carbon, since the acyclic fragments with a tertiary C_3 carbon correspond to the cyclic ones with a C_3 quaternary carbon.

Our population contains 5 fragments with a secondary C_3 carbon, 397 with a tertiary C_3 carbon, and 122 with a quaternary C_3 carbon. One might suppose that the most representative acyclic substructure of this population would integrate the major constraints due to substitution. In other words, 2,2-dimethoxyethane ($\text{CH}_3\text{OCH}(\text{CH}_3)\text{OCH}_3$) or 2,2-dimethoxypropane ($\text{CH}_3\text{OC}(\text{C}-\text{H}_3)_2\text{OCH}_3$) would seem the most suitable model molecules for the purposes of conformational dynamics.

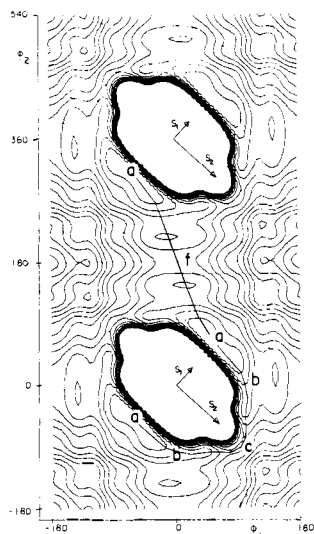


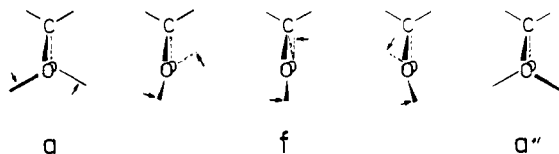
Figure 5. Dimethoxypropane. Level lines determined by the INDO method for an X-ray statistical geometry with $r(\text{CH}_3\text{-O}) = 1.436 \text{ \AA}$; $r(\text{O-C}) = 1.4065 \text{ \AA}$; $\text{CH}_3\text{OC} = 116.165^\circ$; $\text{OCO} = 111.500^\circ$; CH staggered in CH_3OCO . Contour intervals are at $10^{-3}u_a = 0.627 \text{ kcal/mol}$.

However, the acyclic fragments with secondary or quaternary C_3 carbon are in better correspondence with the cyclic fragments having a tertiary C_3 carbon. We, therefore, retained 2,2-dimethoxypropane which offers the further advantage of a higher potential symmetry.

(2) Energy Surface. The semiempirical quantum calculations (INDO method¹⁹) on dimethoxypropane, based on statistical values (intermediate distances and bond angles) taken from X-ray data of acyclic $\text{MeOC}(\text{R}_1, \text{R}_2)\text{OMe}$ fragments (R_1 and $\text{R}_2 \neq \text{H}$), reveal the following facts of particular interest (Figure 5).

(a) Interconversion of the two gear-meshed conformers by correlated conrotation (component $S_1 = (\phi_1 + \phi_2)/2^{1/2}$) is excluded because the barriers involved are too strong.

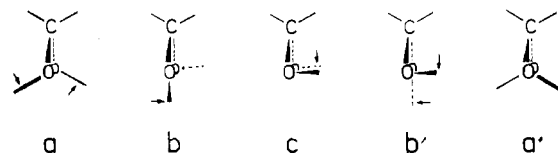
(b) Among the possible interconversion pathways, one is a lateral disrotatory pathway afa'' following the S_2 disrotatory component.



This pathway is similar to that shown by Mislow and co-workers²⁶ for compounds which have in common the *gem*-6 acyclic substructure $\text{C}_3\text{CC}_{\text{sp}^2}\text{CC}_3$. It differs from the lateral crystallographic pathway $adeb''a''$ which should be considered as a deformation of the theoretical pathway. (Unlike the theoretical pathway, the crystallographic pathway $adeb''a''$ alone is not symmetrical and does not satisfy—in symmetric molecules—the principle of Microscopic Reversibility.)

(c) The other interconversion pathway is a particular mechanism involving several steps. (1) A correlated disrotation (ab step) brings one of the Me groups into a position ($\phi_1 = 100^\circ$) of weak interaction with the other Me group. (2) In a stepwise rotation ($bc'b'$ step), the second Me group is blocked in turn in a position minimizing interaction ($\phi_2 = 100^\circ$); then the first moves alone (cb' step) in a direction opposite to that previously adopted. (3) A new and final correlated disrotation ($b'a'$) terminates interconversion. The global result is a conrotation.

Following the gear analogy, we can consider the two OCH_3 rotors as two intermeshed cogwheels. They first undergo a gear effect (correlated rotation ab). Then one of the two wheels escapes (bc). After that, the other wheel also escapes (cb'). Finally, the



two intermeshed wheels undergo another correlated disrotatory process ($b'a'$).

Although this mechanism involving several steps, some correlated and others noncorrelated, appears at first fairly original, one must not forget that the borderline between correlated and non-correlated rotations is not clearly defined. Indeed, in other systems, one of the torsion angles, ϕ_1 , for example, might vary slightly, while the other torsion angle, ϕ_2 , might vary significantly.

(3) Optimization. As confirmed by INDO optimization on 18 structural parameters (bond lengths, bond angles, etc.) interconversion energies are similar for the two pathways: the peripheral pathway needs 1.58 kcal/mol and the lateral disrotatory pathway needs 1.37 kcal/mol.

IV. Concluding Remarks. Monitoring Structural Effects: Electronic and Steric Factors

As clearly shown in the global distribution of Figure 3, many fragments reveal the anomeric effect for only one oxygen (ϕ_1 or $\phi_2 \approx 60^\circ$). In quadrants 1 and 3, some fragments reveal a good anomeric effect for both oxygens ("a" conformers) but this is not the case for any fragment in quadrants 2 and 4 because corresponding structures ($\phi_1 = -\phi_2 = \pm 60^\circ$) are sterically destabilized.

More generally, the emptiness of the central area underlines the destabilization of any conformation in which the interaction of two alkoxy groups is too strong. In particular, all C_2 structures with values $\phi_1 = \phi_2$ from 0° to 45° (S_1 conrotatory axis) and all C_s structures with $\phi_1 = -\phi_2$ and $|\phi_i|$ from 0° to 80° (S_2 disrotatory axis) as well as structures with a locally dissymmetrical COCOC conformation—one $\phi_i \approx 0^\circ$, the other less than 100° —(ϕ_1 or ϕ_2 axis) are all forbidden. These forbidden structures are clearly due to critical distances between the alkyls or the alkoxy groups: all things being otherwise equal (bond angles and bond lengths), these critical distances, in order to be avoided, require smaller torsions for a structure of C_2 symmetry than for a structure of C_s symmetry.

Parallel to these crystallographic observations, we must note that the modest interconversion energies (1.58 and 1.37 kcal/mol) are roughly comparable to the rotation barriers calculated for CH_3OH (1.21 kcal/mol) and CH_3OCH_3 (1.28 kcal/mol) slightly substituted molecules with similar electronic effects, while the higher energies of transition states (9 and 4.6 kcal/mol) observed along the forbidden conrotation pathway emphasize the importance of interactions between nonbonded atoms.

Does the anomeric effect lower the rotation barrier as shown in an experimental example?²⁷ Conflicting observations make it difficult to draw a conclusion. On the one hand, transition states of peripheral and lateral pathways are not anomeric structures. A ground-state stabilized by the anomeric effect should, on the contrary, enhance the rotation barrier.²⁸ On the other hand, it is reduced by minimized steric interactions due to the correlated rotation of methoxy groups and to the relaxation of valency angles all along the interconversion pathways. This barrier is divided in half (1.58 kcal/mol instead of 3 kcal/mol) by this last relaxation of valency angles.

In conformational interpretations and predictions, it is thus clear that transmitting information at a distance implies the simultaneous local minimization of steric interactions between nonbonded atoms and maximization of anomeric stereoelectronic effects.

This study of crystal structures has led to a good assessment of the role played by the anomeric effect and its geometrical parameters. The assessed conversion pathways are of relevant importance as they permit estimates of the conformer populations. All the anomeric fragments are influenced by steric interactions

(26) Nachbar, R. B.; Johnson, C. A.; Mislow, K. *J. Org. Chem.* **1982**, *47*, 4829. Bürgi, H. B.; Hounshell, N. D.; Nachbar, R. B.; Mislow, K. *J. Am. Chem. Soc.* **1983**, *105*, 1427.

(27) Perrin, C. L.; Nuñez, O. *J. Chem. Soc., Chem. Commun.* **1984**, 333.

(28) Deslongchamps, P.; Taillefer, R. *J. Can. J. Chem.* **1975**, *53*, 3029.

with their molecular environments, and further work on these effects is needed to interpret the variety of situations shown in this paper.

It is to be noted that the numerous structures surveyed here belong primarily to carbohydrate chemistry, although many others outside the field have shown the same anomeric-type effect. In other words, the anomeric effect is becoming an important conceptual tool in conformational chemistry. The method used here to evaluate and refine it, so as to then achieve a more precise prediction ability, combines crystallographic data and dynamic fragment information derived from their energy hypersurfaces. Their correlation as suggested by the Mislow-Dunitz-Bürgi proposals is very promising for static and dynamic assessment of

the geometry, the stability, and reactivity of the "anomeric fragments".

Acknowledgment. We express our sincere appreciation to Dr. David G. Watson of the Cambridge Crystallographic Center and to the referees for their helpful, constructive advice.

Registry No. 2,2-Dimethoxypropane, 77-76-9.

Supplementary Material Available: Bibliographic information and reference codes of the data base used, 3D structure of four unusual conformers with one ϕ_i near 0° and the other near 90° (10 pages). Ordering information is given on any current masthead page.

Reductive Fragmentation of 9,9-Diarylflorenes. Concurrent Radical Anion and Dianion Cleavage. Electron Apportionment in Radical Ion Fragmentations¹

Thomas D. Walsh

Contribution from the Department of Chemistry, University of North Carolina at Charlotte, Charlotte, North Carolina 28223. Received April 22, 1986

Abstract: Both radical anions and dianions of 9,9-diarylflorenes cleave an aryl ring after reduction by alkali metals or naphthalenide radical anions in ether solvents. The relative amount of cleavage through each intermediate depends on the alkali metal cation, the solvent, and the presence or absence of 18-crown-6 ether. The tendency for dianion cleavage parallels that for disproportionation of radical anions to dianions and neutral hydrocarbons. Radical anion fragmentation is proposed to proceed via heterolytic cleavage in which electron flow is in the direction which offsets the charge distribution in the radical ion. In the present case, this initially affords 9-arylflorenyl radical and aryl anion, which subsequently undergo electron exchange to form the more stable 9-arylflorenyl anion and aryl radical.

Many types of compounds are known to undergo reduction to radical anions or dianions, followed by cleavage of one or more bonds. This reaction is not limited to the cleavage of C-H or C-C bonds but can be observed in the cleavage of bonds involving a large variety of other elements.² Despite the large number of examples known, in relatively few cases has the mechanism of the reductive cleavage been determined.

The first feature which needs to be addressed is the determination of the species which is responsible for the fragmentation: radical anion or dianion. Some workers have invoked both, under different reaction conditions³ or upon observing different products.⁴ In cases in which the initially reduced radical anion is sufficiently

stable to allow observation of the rate of its disappearance, a first-order kinetic rate law establishes its dissociation. However, in many cases a second-order rate law has been observed, and several other radical anion mechanisms proposed, with the rate law interpreted as involving dimerization⁵ or steady-state concentrations of a reversibly formed intermediate⁶ or explained by using ion-pair association arguments.⁷ Several authors have advanced arguments in favor of radical anion⁸ or dianion^{8c,9a,10} dissociation without determining the rate law.

Dianion intermediacy has been invoked in cases in which the radical anion is observed to be stable, but further reduction produces cleaved products.⁹ It has also been required in studies in which a second-order rate law is accompanied by an inverse dependence of the rate on the concentration of unreduced starting material, as required by the mechanism shown in Scheme I (counter ions omitted for simplicity), in which dianion is produced

(1) Preliminary reports: 186th National Meeting of the American Chemical Society, Washington, DC, August 1983, *Abstracts of Papers*, ORGN-26. 35th Southeastern Regional Meeting of the American Chemical Society, Charlotte, NC, November 1983, *Abstracts of Papers*, p 120.

(2) (a) Schlosser, M. *Angew. Chem., Int. Ed. Engl.* **1964**, *3*, 287-306, 362-373. (b) Perrin, C. L. In *Progress in Physical, Organic Chemistry*; Cohen, S. G., Streitwieser, A., Jr., Taft, R. W., Eds.; Interscience: New York, 1965; Vol. 3, pp 165-316. (c) Garst, J. F. *Acc. Chem. Res.* **1971**, *4*, 400-406. (d) Staley, S. W. In *Selective Organic Transformations*; Thyagarajan, B. S., Ed.; John Wiley & Sons: New York, 1972; Vol. 2, pp 309-348. (e) Petrov, E. S.; Terekhova, M. I.; Shatenshtein, A. I. *Russ. Chem. Rev. (Engl. Transl.)* **1973**, *42*, 713-724. (f) Holy, N. L. *Chem. Rev.* **1974**, *74*, 243-277. (g) Rossi, R. A.; de Rossi, R. H. *Aromatic Substitution by the S_{RN1} Mechanism*; American Chemical Society, Washington, 1983. (h) Todres, Z. V. *Tetrahedron* **1985**, *41*, 2771-2823. Also, most of the references cited in this paper describe reductive bond cleavages.

(3) Remers, W. A.; Gibb, G. J.; Pidacks, C.; Weiss, M. J. *J. Am. Chem. Soc.* **1967**, *89*, 5513-5514.

(4) Kiesele, H. *Angew. Chem., Int. Ed. Engl.* **1983**, *22*, 254; *Angew. Chem. Suppl.* **1983**, 210-221.

(5) Kopping, M. D.; Woolsey, N. F.; Bartak, D. E. *J. Am. Chem. Soc.* **1984**, *106*, 2799-2805.

(6) Ito, O.; Aruga, T.; Matsuda, M. *J. Chem. Soc., Perkin Trans. 2* **1982**, 1113-1115.

(7) Tabner, B. J.; Walker, T. *J. Chem. Soc., Perkin Trans. 2* **1981**, 1295-1297, and previous papers in the series.

(8) (a) Walsh, T. D.; Ross, R. T. *Tetrahedron Lett.* **1968**, 3123-3126. (b) Walborsky, H. M.; Aronoff, M. S.; Schulman, M. F. *J. Org. Chem.* **1971**, *36*, 1036-1040. (c) Testaferri, L.; Tiecco, M.; Tingoli, M.; Chianelli, D.; Montanucci, M. *Tetrahedron* **1982**, *38*, 3687-3692. (d) Patel, K. M.; Baltisberger, R. J.; Stenberg, V. I.; Woolsey, N. F. *J. Org. Chem.* **1982**, *47*, 4250-4254.

(9) (a) Eargle, D. H., Jr. *J. Org. Chem.* **1963**, *28*, 1703-1705. (b) Elschenbroich, C.; Gerson, F.; Reiss, J. A. *J. Am. Chem. Soc.* **1977**, *99*, 60-64.

(10) Grovenstein, E., Jr.; Bhatti, A. M.; Quest, D. E.; Sengupta, D.; VanDerveer, D. *J. Am. Chem. Soc.* **1983**, *105*, 6290-6299.